Bendable large-mode-area fiber with non-circular cores

JUNHUA JI,[1] HUAIQING LIN,[2] RAGHURAMAN SIDHARTHAN,[1] DARYL HO,[1] YANYAN ZHOU,[1] JOHAN NILSSON,[2] SEONGWOO YOO[1,*]

[1]Shool of Electrical and Electronic Engineering, Centre for Optical Fibre Technology, The Photonics Institute, Nanyang Technological University, 639798, Singapore
[2]Optoelectronics Research Center, University of Southampton, Southampton SO17 1BJ, U.K
*Corresponding author: seon.yoo@ntu.edu.sg

Received XX Month XXXX; revised XX Month, XXXX; accepted XX Month XXXX; posted XX Month XXXX (Doc. ID XXXXX); published XX Month XXXX

We investigate mode area scaling and bending performances of a Yb-doped large-mode-area fiber with an elongated non-circular core. Such fiber can be bent in the plane of its short axis to suppress bending effects such as mode area reduction and mode profile distortion. Meanwhile, the other orthogonal axis can be stretched for mode area scaling. Calculations show that for fibers with same mode area, the higher aspect ratio between the long axis and short axis the fiber has, the less sensitive the fiber will be to bending effects. However, mode area scaling is limited by the increased beat length between the fundamental mode and the second order mode, leading to mode degeneracy at higher aspect ratios. Within 100 mm beat length, the fundamental mode area is scalable to 3,000 μm² in a bent fiber. To facilitate fundamental mode operation, we study mode-selective gain through confined doping. Thanks to the small bending distortions, the confined-doping approach works well in the bent large-mode-area fiber. Besides, the advantage of tandem pumping is also discussed in terms of preferential modal gain.
A non-circular core fiber with a 41 μm short axis and 120 μm long axis was fabricated in-house. We evaluated the fiber in a linear laser cavity pumped by a 975 nm laser diode. The maximum output power obtained was 191 W with slope efficiency of approximately 67% with respect to launched pump power. The output signal has good beam qualities with M^2 of ~1.5 and ~3.1 respectively, along short and long axis.

OCIS codes: *(140.3510) Lasers, fiber; (140.3280) Laser amplifiers; (060.2310) Fiber optics.*

http://dx.doi.org/10.1364/AO.99.099999

1. INTRODUCTION

Large-mode-area (LMA) Yb-doped fibers are commonly used in fiber amplifiers and lasers for generation of high power and high energy radiation [1]-[2]. Thanks to the large effective area of the fundamental mode (FM), the onset of undesirable nonlinear effects and catastrophic optical damage can be avoided [3]-[4]. With the increase of the core size, the output beam is expected to become multi-moded with degraded beam quality. To maintain good beam quality at the output, high-order-modes (HOMs) are suppressed by both experimental techniques and specialty fiber designs. For example, in a conventionally designed few-moded fiber, HOMs can be filtered out through bending [5] and the FM can be selectively excited at the launch [6]. For both cases, the effective area of the FM is limited to about 1000 μm² since the effective-index difference between the FM and HOMs becomes smaller as the mode area increases. This leads to mode mixing and nullifies the mode-selective bending loss scheme for single mode operation [5]. Various specialty LMA fiber designs are reported to further extend the core size while preventing unwanted HOMs by mode-selective gain, e.g., through selective doping [7], or mode-differentiated losses, e.g., chirally-coupled core (CCC) fibers [8], leaky channel fibers (LCFs) [9], large-pitch photonic-crystal fibers (LPFs) [10], and multi-trench fibers (MTFs) [11]. However, fiber bending often compromises the mode area scalability and the effects of bending are recognized as an important limiting factor for mode area scaling [12]. Bending a fiber not only squeezes the effective mode area and consequently reduces the threshold powers for nonlinear scattering and material breakdown, but also shifts the mode profile toward the cladding, and alters the mode overlap with the doped gain area. This can deteriorate the gain ratio between FM and HOMs. Hence, it is necessary to develop bendable LMA fibers for many applications including high energy scaling and high energy beam delivery.

There are several approaches that alleviate at least some of the detrimental bending effects. One example is a parabolic refractive index profile with modified cladding index structure with mode area of 1000 μm² or higher [13]. In addition, an all-solid photonic bandgap fiber is reported to be bendable up to an effective area of 920 μm² [14]. Alternatively, an asymmetric core was investigated as a bendable LMA

design. The semi-guiding high-aspect-ratio core (SHARC) is another proposed bendable LMA design [15]. One disadvantage with this approach is that the fiber has two sets of core-cladding boundaries and uses a very high aspect ratio (AR) (> 30:1). This makes fabrication very challenging. More recently, a ribbon core fiber combining 13 small circular cores, parallel in a line, was fabricated through a stack-and-draw technique. The fiber was used to amplify a single higher-order mode (HOM) [16] for power scaling, and FM operation was demonstrated through external mode selection [17]. This improves the beam quality. The ribbon fiber is similar to so-called multicore fibers except that multicores of ribbon fibers are placed in a line so that bending effects are negligible along certain axis.

In this paper, we investigate mode area scaling and bending performances of a non-circular core fiber with simpler fiber structure compared to SHARC fibers and ribbon fibers. Our non-circular core fibers are similar to conventional double-clad fibers except that cores are elongated instead of circular shapes. One shorter axis of the core is defined to suppress bending distortion at a desired maximum bending curvature. Here, we consider the bending radius of 25 cm (or bending curvature of 4 m^{-1}), which is useful for many applications and compatible with industrial packages. Bending effects can be greatly suppressed as long as the short core axis is in the bending plane. Meanwhile, there is a degree of freedom to stretch the orthogonal axis and scale the mode area by forming an elongated core resilient to bending distortion. We found that the mode scaling of such fibers is limited by the beat length (BL) between the FM and HOMs. Still, in a fiber bent to 25 cm radius, the fundamental mode area can be scaled to about 3000 μm^2 with a workable BL. Furthermore, we investigated the performances of such fibers together with other techniques, i.e., confined doping and tandem-pumping [18] in our simulations. As show in [18], tandem-pumping helps to ensure most pump power converted to the fundamental mode rather than HOMs, and therefore, a good beam quality at the output. By contrast, confined doping can be less effective in circular LMA fibers due to bending distortion, if we rule out complicated pre-compensated refractive index profiles [19]. On the other hand, thermally driven transverse mode instability (TMI) arises at very high output power and degrade the output beam quality. In our pervious investigation of TMI in non-circular core fibers [20], we find that interestingly, TMI is determined by a long core axis rather than a short axis. Thus, their power transfer strength despite its better heat dissipation is stronger than circular cores in a same effective mode area, resulting in more significant TMI. Although the TMI threshold of such fibers is not improved, bendable LMA non-circular core fibers can be useful for the generation of high energy sources with moderate average output powers. We focused on obtaining large mode areas in bent fibers.

Based on our analysis, a double-clad non-circular core fiber doped with Yb ions was fabricated in-house with the conventional modified chemical vapor deposition (MCVD) process and a chelate vapor delivery process. The fiber was tested in a linear cavity pumped by a 975 nm laser diode (LD). The highest signal power obtained was 191 W at 296 W launched pump power. The corresponding slope efficiency was 67.2% with respect to the launched pump power. The measured M^2 factors were ~1.56 and 3.11 respectively, along the short and long core axis. The slightly worse M^2 factors along the long core axis is due to a deviation of the short axis from the bending plane.

The paper is organized as below. Section 2 discusses the bending effects, mode scaling and its limitations in bent fibers with non-circular cores. In section 3, both selective doping and tandem pumping are studied in proposed fibers. Both techniques can facilitate fundamental-mode operation, as shown by simulations. The details of the fabricated fiber and the experimental results with this fiber are given in sections 4 and 5, respectively. We then conclude the paper with section 6.

2. THEORETICAL INVESTIGATION ON BENDING EFFECTS IN ASYMMETRIC CORE

In a bent fiber, the mode distribution shifts to the edge of the waveguide structure, and the corresponding mode area is reduced by an amount determined by the bending radius and fiber parameters [12]. The influence of bending on the FM effective area for different core aspect ratios (ARs) together with a circular core is presented in Fig. 1. The core area is 10,200 μm^2, and the wavelength is 1080 nm in all cases. The core numerical aperture (NA) is assumed to be 0.06, which is achievable with MCVD with good yield and is commonly found in LMA fibers. The modes are calculated with COMSOL, using standard conformal mapping to treat the bending [21]. The FM areas of all fibers are slightly over 5,000 μm^2 when straight (e.g. 5,300 μm^2 in the circular core). The effective mode areas in the bent fibers are scaled by their straight-fiber values. The mode profiles in cores with ARs of one and ten are shown, too.

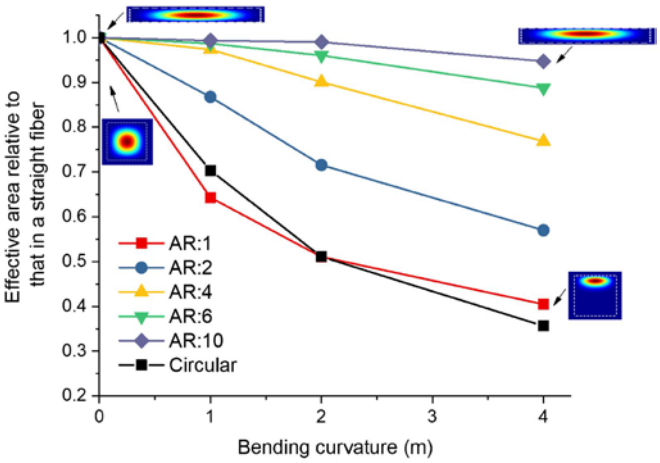

Fig. 1. Dependence on bending (in the direction of the short axis) of the effective areas of the FM in fibers with different ARs. FM profiles for selected straight and bent fiber are also shown. A circular core with the same size is also plotted for comparison.

Similarly to the same size circular core, the mode area in the square core, i.e., with AR of one, quickly shrinks in the bent fiber. Figure 1 shows that at 4 m^{-1} bending curvature, the effective area becomes only 41% of its straight counterpart. As the AR increases, the mode area shrinks less. In the fibers with the AR of six or above, the FM-area remains larger than 90% of the straight-fiber value at 4 m^{-1} bending curvature. In addition to the mode-area shrinkage, the shift of the mode profile will change its overlap with the gain region, and degrade the gain of the FM relative to other modes. In the square core, the FM's intensity peak shifts about 37% relative to the core size. This makes mode-selection through confined doping ineffective. By contrast, the peak only moves 12% of the core at AR of 10, and 20% at AR of 6. We also note that if the fiber is bent in the orthogonal direction, i.e., with the long axis of the core in the bending plane, then the fiber with higher aspect ratio is more sensitive to the bending.

The core with AR of six has 41 μm short-axis height in Fig. 1. As the bending performance is determined by the short axis when bent in the short axis plane, it is anticipated that significance of bending distortion would be remained in the same level regardless of the long-axis size, or the ARs. In other words, the mode shrinkage and its peak shift are invariant as long as the short axis is fixed at 41 μm at the 25 cm bending

radius. This is investigated in Fig. 2 for AR in the range of 1–50 with a fixed short axis size of 41 μm. The mode shrinkage is indeed maintained around 10% for all ARs, including the square core. Furthermore, the mode peak shift is kept below 20% relative to the core height. The mode intensity profiles along the short axis at all ARs are shown in the inset of Fig. 2. They all overlap and cannot be differentiated.

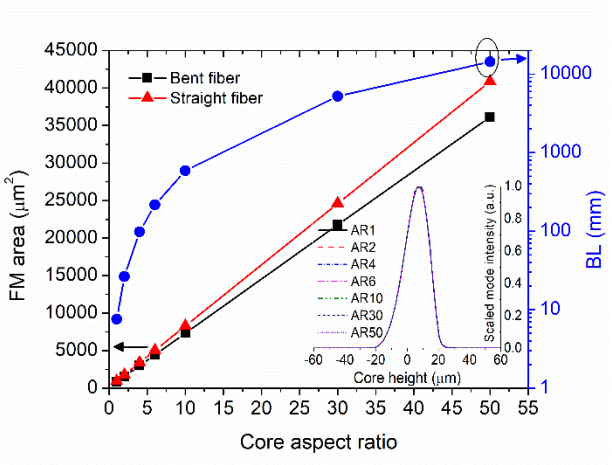

Fig. 2. Mode area scalability of a rectangular core fiber with 41 μm core height in the short axis at different ARs. The bent fiber has a curvature of 4 m^{-1}. The beat length between the FM and the first HOM is also shown. Inset: mode intensity profiles at the investigated ARs along the short axis for bent fiber.

As shown in Fig. 2, the mode area scales linearly with core AR at a fixed short axis. However, the increased AR also increases the BL between the FM and the first HOM as shown in Fig. 2. The BL reaches even 1 m for the AR of 30. The BL of 1 m corresponds to modal index difference of 10^{-6}. Then, eventually the modes are effectively degenerate, and become indiscernible. Hence, mode area scaling in a rectangular core should consider beat length as well as the bending effects for robust FM operation. We will assume that a BL of ~ 100 mm is workable for single mode operation. A BL which we estimate ~ 100 mm has been demonstrated in a straight LPF with 26 mJ output pulse energy, 100 W average power and nearly diffraction-limited output beam [2]. In another experiment with a coiled step-index fiber with a BL that we estimate to ~126 mm, the output beam was multimoded with measured M^2 of ~6.5 [22]. However, the beam can be improved, perhaps even to diffraction-limited quality, through techniques such as tandem pumping and confined doping to be discussed in the next section. Therefore, we target similar BL, i.e., 100 mm, in our bent non-circular core fibers. This then limits the AR to 4, corresponding to the FM area slightly above 3,000 $μm^2$ at 1080 nm in a bent fiber. We note that the BL selection does not promise a FM operation, but rather makes the FM mode as well as other HOMs more distinguishable. The FM operation is promoted via a confined doping scheme as discussed in the following section. A selective bending loss [1, 5] would add further modal discrimination albeit somewhat limited in the considered BL [22].

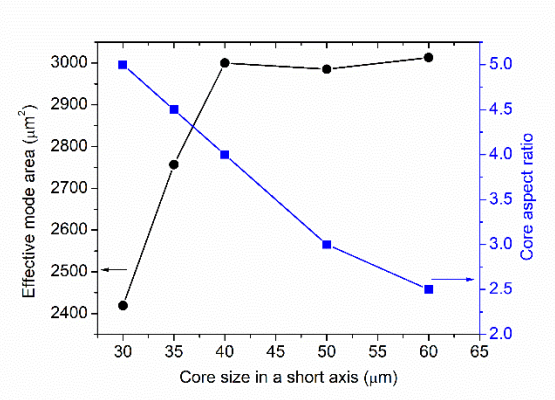

Fig. 3. Achievable mode area at different short-axis core sizes. The core aspect ratio required for the mode area is presented as well. The fiber is bent at 4 m^{-1} bending curvature.

We investigate mode area scalability in various short-axis core sizes within the BL constraint as presented in Fig. 3. With the increasing short axis size, the allowed core AR within the BL constraint is reduced. Furthermore, there is no considerable benefit to enlarge the short axis above 40 μm in terms of mode area scaling. In fact, the larger short axis core experiences more significant bending distortion at the target bending curvature. For instance, a 50 μm short axis core suffers 23% of mode shrinkage and 24% of peak shift which are worse than the 41 μm short axis core. Consequently, the core with 41 μm short axis with an AR of 4 well represents the achievable mode area at the bending curvature of 4 m^{-1}.

3. FUNDAMENTAL MODE SELECTION BY CONFINED DOPING AND TANDEM PUMPING

The low bend-distortion in the rectangular core fiber facilitates the use of confined doping to preferentially amplify the FM. It is also known that tandem pumping can reduce HOM gain when the FM gain is saturated [18]. We theoretically study the benefit of confined doping and tandem pumping in the rectangular core fiber. We follow the theoretical analysis in [18] to investigate the modal gain ratio when the FM gain is assumed saturated with an average Yb excitation level across the signal mode of 3%. For the high-power devices we consider, the pump and stimulated-emission rates dominate over the spontaneous-emission rate. Amplified spontaneous emission (ASE) is not taken into account for the ion excitation, which is assumed to be determined by only the pump and signal power. In this case, if the ratio Ps / Pp is constant along the fiber, the excitation level will not change along the fiber. This situation is a good approximation of a saturated amplifier with counter-propagating pump and signals, if the operating pump absorption and signal gain are approximately equal. Then, in the absence of loss, the number of pump photons will be equal the number of signal photons in each cross-section of the fiber.

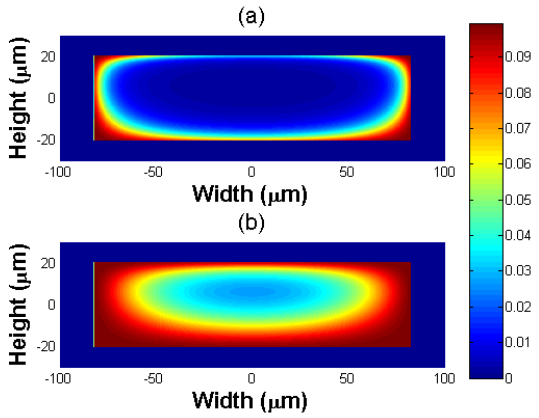

Fig. 4. Fractional Yb excitation level inside uniformly doped fiber core bent at 4 m^{-1} bending curvature. The core height is 41 μm. Pump wavelength (a) 915 nm and (b) 1020 nm. The core aspect ratio is 4:1 with 41 μm core height. White lines indicate the core boundary.

Figure 4 shows the excitation level in a rectangular core fiber, uniformly Yb-doped throughout the core, when pumped at two typical wavelengths, i.e. 915 nm for LD pumping, and 1020 nm for tandem pumping. The signal wavelength is assumed at 1080 nm. The cladding area is adjusted for an average fractional excitation of 0.03. It leads to 0.96 dB/m of pump absorption corresponding to Yb ion concentration of 2% by weight in a P-doped silica core. In a P:Yb silica fiber, photodarkening can be negligible [23]. The same pump absorption level is obtainable in other host materials, e.g. alumino-silicate glass by controlling the doping level and cladding size. In accordance with the analysis in Sect. II, the fiber core has a 0.06 NA, a 4:1 AR, and a 41 μm short axis size. The white lines in Fig. 4 show the edge of the core. The fiber is bent to 4 m^{-1} curvature. As expected from [18], the Yb ion inversion is more uniformly distributed across the core under 1020 nm pumping compared to that with diode-pumping at 915 nm. The inversion in the edge under 915 nm pumping is up to 24 times larger than the average inversion level, which can result in unwanted high gain in HOMs. On the other hand, under 1020 nm pumping, the highest edge inversion is only three times higher than the average inversion. Hence, in a uniformly doped rectangular core, tandem pumping can help avoid undesired high gain in HOMs.

The ratio between the FM gain and the highest gain in HOMs is calculated for different fractional doping areas, with LD pumping at 915 and 975 nm, and tandem pumping at 1020 and 1030 nm. The same core parameters and the same bending are assumed as in Fig. 4. The results are shown in Fig. 5. It is clear that the confined doping works well, and the gain ratio is improved by reducing the confined doping ratio at all investigated pumping wavelengths. The FM gain becomes higher than that of any HOM for doping area ratios in the range of 0.1 – 0.4 for both tandem-pumping and diode-pumping. For larger doped areas, the HOM gain exceeds the FM gain in all pumping schemes. Nonetheless, the tandem pumping is found more favorable in terms of lower gain ratio. In the uniformly doped core, the highest HOM gain is only 1.7 and 2.3 times larger than the saturated FM gain of 0.96 dB/m at 1030 nm and 1020 nm pumping wavelengths, respectively.

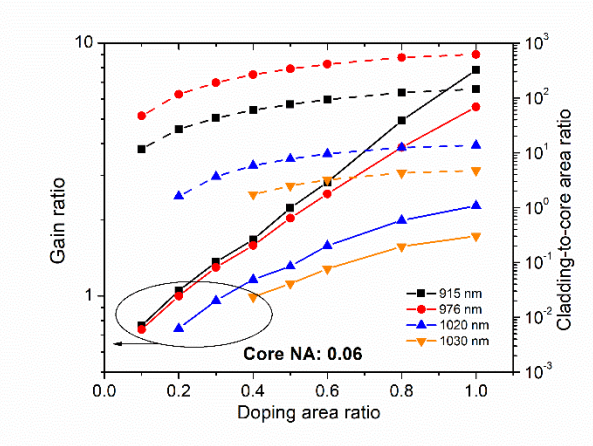

Fig. 5. Calculated gain ratio between the HOM with highest gain and the FM at different doping area ratios for different pumping wavelengths. The core NA is 0.06. Bent fiber with 0.25 m^{-1} curvature is assumed. The required cladding-to-core area ratio is also plotted for the assumed 0.03 inversion level.

We note that the tandem pumping should be accompanied with a small cladding-to-core area ratio as shown in Fig. 5. This requirement can be fulfilled with high brightness pumping sources such as fiber laser. The calculation stops when the required cladding-to-core area ratio becomes smaller than one because it is practically unachievable. The pump area is adjusted to different doping ratios to keep the same average excitation level of 3% for all cases. When the doping ratio becomes smaller, a smaller cladding-to-core area ratio is necessary.

We now consider the benefit and practicability of the confined doping in the LD pumping. The gain ratio improves nearly an order of magnitude by introducing the confined doping as shown in Fig. 5. With 0.1 of the doping ratio, the FM sees the highest gain among the supported modes. However, this requires cladding-to-core area ratio of 10 at 915 nm pumping or 50 at 976 nm pumping to reach 0.96 dB/m gain. With the doping area ratio of 0.2, the FM gain is still higher than HOMs under 976 nm pumping, and its required cladding-to-core area ratio is 110, which is practical for aspects of fabrication as well as available pump brightness.

We next extend our investigation to a larger core NA to see if rectangular cores with confined doping is useful for highly doped fibers. In addition to the Yb-doped fibers, Tm-doped fibers are often highly doped to allow efficient 2-for-1 cross-relaxation [24]. The highly doped core inevitably raises a refractive index, which subsequently requires compensation of the raised index to control beam quality. A pedestal design [25] or an equi-molar Al:P [26] core were proposed in prior works. The confined doping could be an alternative option for controlling the beam quality in a raised refractive index. To investigate this possibility, a core NA of 0.15 is chosen, which allows us to increase the short-axis size to 45 μm without significant bending distortion. This short-axis core size keeps the FM distortion small, i.e. 87% of the mode area is preserved and the mode peak shift is only 12% of the short-axis core size. With the core AR of 4, the beat length becomes 119 mm, and further area scaling is not considered. The same bending curvature as in Fig. 4 is assumed as before.

The gain ratio calculated for the fiber with core NA 0.15 presented in Fig. 6. For the AR of 4, the FM area is 3,330 μm^2. It is found that the confined doping is effective to control the gain ratio at the bending. Similar to Fig. 5, under the LD pumping, the gain ratio is improved by an order of magnitude from uniform doping to 0.1 doping area ratio. Again,

the tandem pumping improves the gain ratio in the high NA core as observed in the 0.06 core NA.

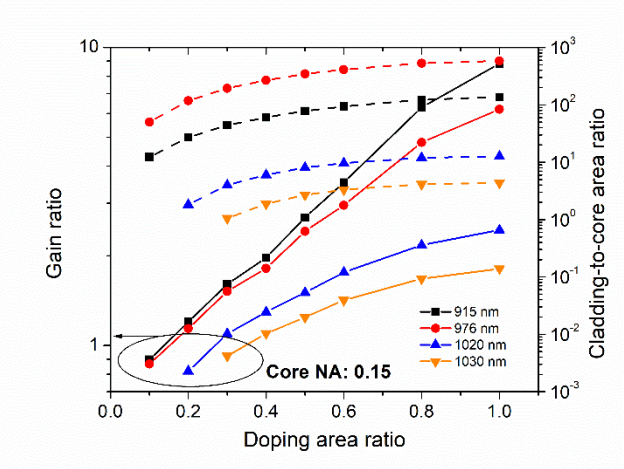

Fig. 6. Calculated gain ratio between the HOM with highest gain and the FM at different doping area ratios under various pumping wavelengths. The core NA is 0.15. Bent fiber with 0.25 m^{-1} curvature is assumed. A required cladding-to-core area ratio is also plotted for the assumed 0.03 inversion level.

The confined doping looks promising as long as the fiber bends in the intended plane of the shorter axis. It is interesting to see its performance when the bending plane becomes out of the intended one. The effect of the bending orientation offset is investigated at 915 and 1020 nm pumping. Figure 7 shows the calculated bending distortion with the offset angle between the bending plane and the core short axis. The fiber parameters are the same as in Fig. 5. The performance is notably affected by the orientation deviation. The FM area reduces to 67% of its original value for an angle of 3°. The gain ratio is also impaired by the angle offset, although the impact becomes weaker with the tandem pumping than with LD pumping. With the doping area ratio of 0.2, the gain ratio becomes 3.9 times at 915 nm pumping with a 3° offset, compared to 1.5 times at 1020 nm pumping. In the uniformly doped core, the gain ratio becomes less sensitive to the bending angle offset although its gain ratio is always larger than the confined doping case.

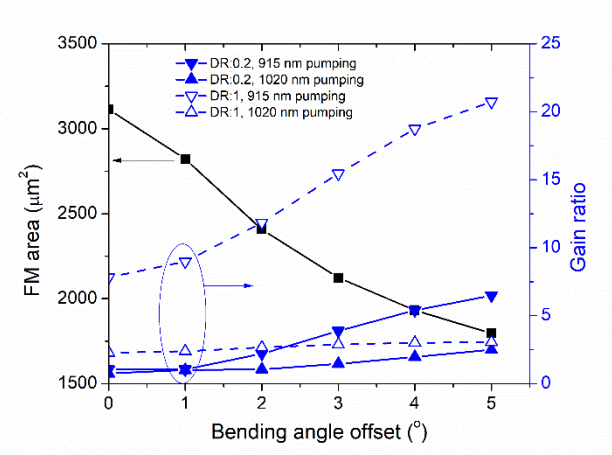

Fig. 7. Bending performance against bending angle offset. The fiber parameters are the same as in Fig. 4. DR: Doping area ratio.

4. FIBER FABRICATION

We fabricated fibers with a laterally stretched core and confined doping. Fiber preforms were fabricated by the conventional MCVD process. We used a chelate vapor delivery process to incorporate Yb ions in the preforms. The circular symmetry of the preforms became broken while undergoing post-processing such as side-milling by ultrasonic milling machine and subsequent fire polishing in the MCVD lathe. The milled cladding gets rounded during the high temperature fire polishing step. Such cladding transformation reshapes the core to a non-circular stretched shape. The post-processing can be repeated to reach a desired dimension. We were able to control the core aspect ratio in the range from 3:1 to 20:1 in a double-clad structure by applying the post-processing and glass compositions with different viscosity.

After the post-processing, cladding was milled to double D-shape to improve pump absorption as well as control the bending axis. When attempted to bend, the double D-shaped fiber naturally bends in the intended shorter axis plane as the fiber is thinner along the shorter axis.

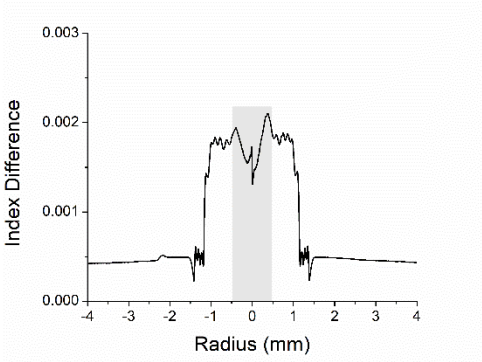

Fig. 8. Refractive index profile of confined doping fiber preform. The shaded area indicates the Yb doped region. Its doping area ratio is 0.2.

Output of several fabricated preforms and fibers, one was selected for further experiments. Figure 8 represents the refractive index profile (RIP) of the preform before core shaping. The Yb ions are doped only in the center of the core as indicated as a shaded area. The doping area ratio is 0.2. The core refractive index is raised to 0.066 of NA. We noticed a slight refractive index deviation of 0.0003 between the doped and the undoped region in the core. The slight deviation could be further reduced through MCVD process optimization. We introduced a slight refractive index dip in the center to compensate the index deviation. A stretched core fiber was drawn to a core size of 41 and 120 μm in a short and long axis, respectively. The fiber was coated with a low refractive index polymer to form a pump waveguide in the cladding with nominal NA of 0.45. A microscopic image of the fiber is shown in Fig. 9. The small signal absorption of the fiber was measured to 1 dB/m at 976 nm. An estimated Yb concentration is 0.2 wt%. We used this fiber for laser efficiency test.

This fiber was fabricated according to the design suggested by our simulations in the previous two sections. Thus, with the 41 μm short axis, the fiber can be bent to a radius of 25 cm Fig. 2. With the core AR of 3, the fabricated fiber has BL between FM and close HOM is around 58 mm, shorter than 100 mm. The FM mode area is estimated to be 2,571 μm^2. With the fabricated 0.2 area doping ratio, and the cladding-to-core area ratio of about 100, the FM can see higher gain than HOMs if pumped by 915 nm LDs as shown in Fig. 5.

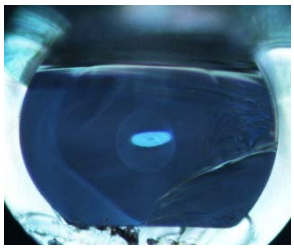

Fig. 9. Fabricated stretched core fibers with a core aspect ratio of 1:3 with 41:120 μm. Its cladding is 770 μm in a long axis.

Ideally, the milled edge of the cladding should be parallel to the longer core axis. However, for the fabricated fiber, the longer core axis is not perfectly parallel to the milled edge of the cladding, which induces a orientation between the intended and actual bending planes. The deviation angle for the fiber used in the experiment is estimated to be ~3º. As discussed in the previous section, the angle deviation can cause beam distortion and therefore degrade the output beam quality. Our experiments described in the next section explore this.

5. LASER EXPERIMENT

Figure 10 shows the schematic diagram of the experimental setup for the laser slope efficiency and beam quality measurements. A 976-nm pump-LD was free-space coupled into a 20 m long fiber through a dichroic mirror (DM). Both ends of the fiber were perpendicularly polished to work as laser cavity mirrors through 4% Fresnel reflections. Thus, the laser output was bi-directional. Wedges were used to sample the forward signal for beam quality measurement, following reflection in another DM. Both DMs have high transmission around 975 nm and high reflection around 1.06 μm.

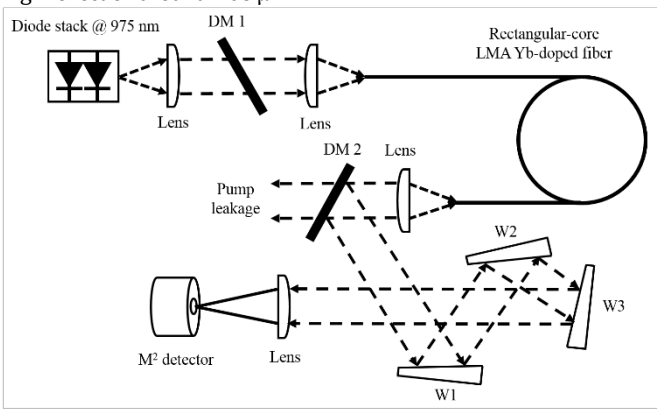

Fig. 10. Schematic of the experimental setup for laser slope efficiency and beam quality measurements. DM: dichroic mirror; W: wedge.

Firstly, the forward laser output power (black squares) and pump residual power (red circles) were characterized with the increase of the pump power as shown in Fig. 11. During the measurements, the fiber was bent along its short axis with the bending diameter of 95 cm. As shown in Fig. 11, the forward signal power increases nearly linearly with the pump power. The small deviation from linearity may be explained by the variation in pump absorption, which in turn is caused by a drift in pump wavelength. The highest power of the forward signal was 191 W, obtained at 296 W launched pump power. The output power is only limited by the available pump power. There is no sign of the onset of nonlinear effects to limit the output signal power. This is confirmed with the laser output spectrum measurement at full power, which is given in Fig. 12. The lasing spectrum extends from 1040 nm to 1090 nm. With higher pump power, the output signal power can be expected to be further increased. The slope efficiency against the launched pump power is 67.2%. Note that the leaked pump power dropped when the launched pump power exceeded 150 W. This is because the pump wavelength drifts to longer wavelengths with higher absorption when the pump power increases.

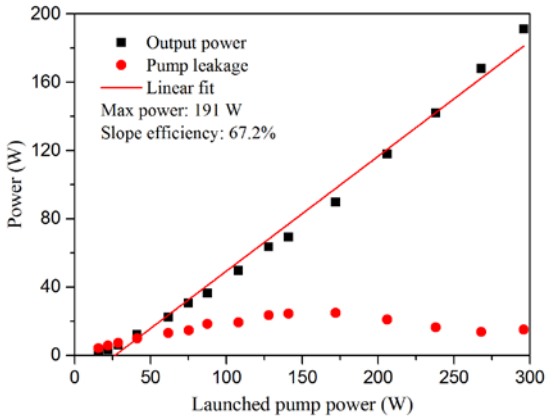

Fig. 11. Output powers of forward signal and residual pump vs. launched pump power.

We also measured the beam quality of the output signal with a Thorlabs beam profiler (Model no: BP104-IR), adopting the 4σ method and the hyperbolic fit algorithm of the profiler. The fiber was bent along its short axis with 90-cm bending diameter. Figure 13 shows the measured results of the M² factors at different launched pump powers. The average values of M² factors along short axis (or x-axis) and long axis (or y-axis) are 1.56 and 3.11, respectively.

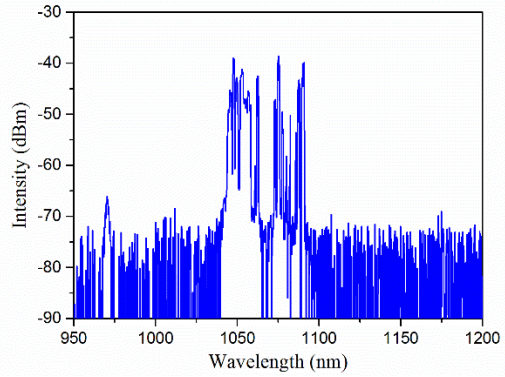

Fig. 12. Laser output spectrum at 191 W signal power with 1.0 nm resolution.

The relationships between fiber parameters, normalized frequency, V and M^2 factor are given by the following two equations if all core modes are equally excited:

$$V_x = \frac{2\pi r_x \cdot NA}{\lambda}, V_y = \frac{2\pi r_y \cdot NA}{\lambda} \quad (1)$$

$$M_x^2 = \frac{V_x}{2}, M_y^2 = \frac{V_y}{2} \quad (2)$$

where r and NA are radius and numerical aperture of the fibre core, respectively, and λ is the wavelength. The M_x^2 and M_y^2 of the fiber core are estimated to be 7.99 and 22.21, respectively. Compared to these theoretical values, the measured M² factors are much smaller. The

HOMs are well suppressed, which we attribute at least in part to the confined doping. Therefore, the beam qualities are better than the values given by Eq. (1) and (2) in the case that all modes are equally excited. Even better beam qualities are expected if there is no misalignment between the longer core axis and the milled edge of the cladding.

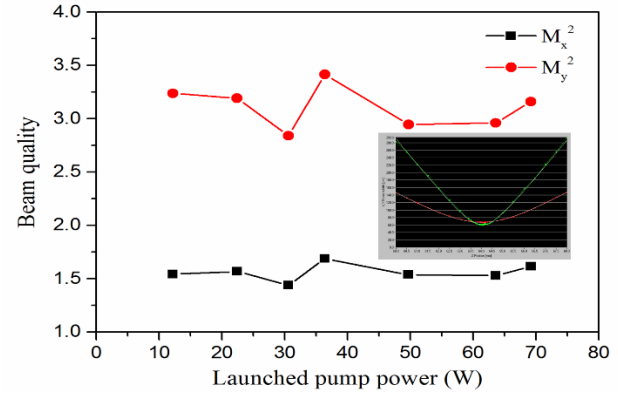

Fig. 13. Measured beam quality factor M^2 at different pump powers. Inset: M^2 fitting curve at the maximum power

The beam qualities were also measured at 60 cm and 110 cm bending diameters to further verify whether the designed fiber is capable of suppressing the bending effects. A 19 m long fiber was used cut back from the 20 m long piece. The fiber was bent with diameters of 60 cm, 90 cm and 110 cm, respectively, and M^2 factors were measured. The measured results are plotted in Fig. 14. Once again, when the bending diameter is fixed, the beam quality factors along both x and y axes almost remain same with the increase of launched pump power. The M^2 factors are very close to each other at 90 cm and 110 cm bending diameters. At the same laser output power, the beam quality with 110 cm bending diameter is slightly better than that with 90 cm bending diameter. When the fiber was tightly bent at 60 cm bending diameter, the beam qualities became worse. For example, M^2 factors along x-axis and y-axis degraded from 1.753 to 2.116 and from 3.442 to 4.449 with a bending diameter reduced from 110 cm to 60 cm. The 60 cm bending diameter is close to the designed minimum bending diameter, i.e., 50 cm.

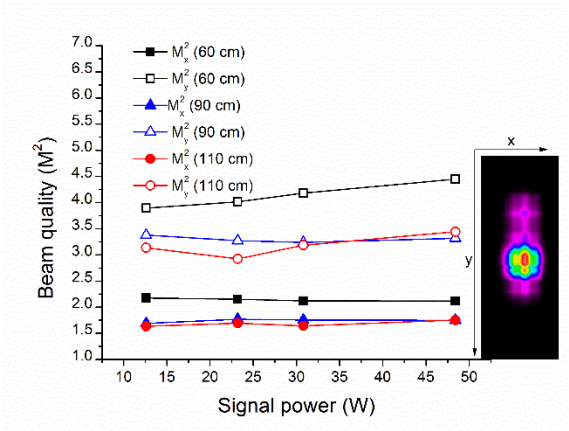

Fig. 14. Beam quality factor M^2 at different signal powers with a 19 m fiber length.

The rectangular-core fiber is designed to bend along the short axis, and deviations from this can induce considerable bending distortion. The effect of the bending distortion with the deviation has been simulated and is given in Fig. 7. It shows that the FM area with 3º angular error is reduced to 67% of its mode area bent in short axis plane. The misalignment angle between the core and short axis is estimated to be 3º. The inset of Fig. 14 shows the mode distribution at the maximum output power with 90 cm bending diameter. That means the misalignment between the core and the cladding axes of this fiber sample will enlarge the bending distortions. With even smaller bending diameter, e.g., 60 cm, more power will be seen in the side lobe. The beam quality along the long core axis will further degrade. This bending induced distortion might also explain the somewhat limited slope efficiency in Fig. 11. The post-processing introduced a slight twist of core in a preform, and this could not be recovered. However, we believe that employing 3D computer numerical control (CNC) machining for the D-shaping will be helpful to minimize the misalignment between the core and cladding. The CNC allows us to shape a preform vertically, with precise tracking of the core axis along the preform. The milled edge of the cladding can then be more accurately aligned with the longer core axis along the whole piece. We also note that the asymmetric core may induce a polarization effect, particularly for HOMs [27]. This could be examined in other context.

6. CONCLUSION

Non-circular elongated-core fibers are investigated as a bendable LMA design. We propose a design approach to reach the maximum achievable mode area at a desired bending curvature, under the constraint of a maximum beat length between FM and HOM. A mode area of 3,000 μm^2 is found achievable at 4 m^{-1} of bending curvature within 100 mm beat length. Selective doping in the rectangular core is found effective to promote single mode operation in the 3,000 μm^2 mode area. Preferential gain for the FM is ensured at LD pumping as well as tandem pumping. This approach is also effective in high core NA fiber with high rare-earth concentration.

We demonstrated fabrication of the stretched core fiber using the conventional MCVD process in conjunction with post-processing. The core aspect ratio could be adjusted between 3:1 and 20:1. A confined doping was successfully implemented in the stretched core to facilitate FM operation. The fiber exhibited efficient laser performance with 67% of slope efficiency and nearly 200 W output power, only limited by the available pump power. Its beam quality factor was measured about 1.3 and 3.1 respectively along short axis and long axis, indicating HOM excitation during the laser operation. We attributed this HOM excitation to the offset bending angle. Better beam quality factor should be achievable if this deviation-induced bending distortion is avoided.

References

1. Y. Jeong, J. K. Sahu, D. N. Payne, and J. Nilsson, "Ytterbium-doped large-core fiber laser with 1.36 kW continuous-wave output power," Opt. Express **12**, 6088(2004).
2. F. Stutzki, F. Jansen, A. Liem, C. Jauregui, J. Limpert, and A. Tünnermann, "26 mJ, 130 W Q-switched fiber-laser system with near-diffraction-limited beam quality," Opt. Lett. **37**, 1073-1075(2012).
3. D. J. Richardson, J. Nilsson, and W. A. Clarkson, "High power fiber lasers: current status and future perspectives," J. Opt. Soc. Am. B **27**, B63(2010).
4. J. W. Dawson, M. J. Messerly, R. J. Beach, M. Y. Shverdin, E. A. Stappaerts, A. K. Sridharan, P. H. Pax, J. E. Heebner, C. W. Siders, and C. P. J. Barty, "Analysis of the scalability of diffraction-limited fiber lasers and amplifiers to high average power," Opt. Express **16**, 13240(2008).
5. J. P. Koplow, D. A. Kliner, and L. Goldberg, "Single-mode operation of a coiled multimode fiber amplifier," Opt. Lett. **25**, 442(2000).

6. M. E. Fermann, "Single-mode excitation of multimode fibers with ultrashort pulses," Opt. Lett. **23**, 52(1998).
7. J. R. Marciante, "Gain filtering for single-spatial-mode operation of large-mode-area fiber amplifiers," IEEE J. Sel. Top. Quantum Electron. **15**, 30(2009).
8. C. Liu, G. Chang, N. Litchinitser, A. Galvanauskas, D. Guertin, N. Jacobson, and K. Tankala, "Effective single-mode chirally-coupled core fiber," in Advanced Solid-State Photonics 2007 (Optical Society of America, 2007), paper ME2.
9. L. Dong, T. W. Wu, H. A. McKay, L. Fu, J. Li, and H. G. Winful, "All-glass large-core leakage channel fibers," IEEE J. Sel. Top. Quantum Electron. **15**, 47(2009).
10. J. Limpert, F. Stutzki, F. Jansen, H. J. Otto, T. Eidam, C. Jauregui, and A. Tünnermann, "Yb-doped large-pitch fibers: effective single-mode operation based on higher-order mode delocalization," Light: Sci. & App. **1**, 1(2012).
11. D. Jain, C. Baskiotis, and J. K. Sahu, "Mode area scaling with multi-trench rod--," Opt. Express **21**, 1448(2013).
12. J. M. Fini, "Bend-resistant design of conventional and microstructure fibers with very large mode area," Opt. Express **14**, 69(2006).
13. J. Fini and J. Nicholson, "Bend compensated large-mode-area fibers: achieving robust single-modedness with transformation optics," Opt. Express **21**, 19173(2013).
14. F. Kong, K. Saitoh, D. Mcclane, T. Hawkins, P. Foy, G. Gu, and L. Dong, "Mode area scaling with all-solid photonic bandgap fiber," Opt. Express **20**, 26363(2012).
15. J. R. Marciante, V. V. Shkunov, and D. A. Rockwell "Semi-guiding high-aspect-ratio core (SHARC) fiber amplifiers with ultra-large core area for single-mode kW operation in a compact coilable package," Opt. Express **20**, 20238(2012).
16. D. Drachenberg, M. Messerly, P. Pax, A. Sridharan, J. Tassano, and J. Dawson, "First multi-watt ribbon fiber oscillator in a high order mode," Opt. Express **21**, 18089(2013).
17. B. Anderson, G. Venus, D. Ott, I. Divliansky, J. W. Dawson, D. R. Drachenberg, M. J. Messerly, P. H. Pax, J. B. Tassano, and L. B. Glebov, "Fundamental mode operation of a ribbon fiber laser by way of volume Bragg gratings," Opt. Lett. **39**, 6498(2014).
18. C. A. Codemard, J. K. Sahu, and J. Nilsson, "Tandem cladding-pumping for control of excess gain in ytterbium-doped fiber amplifiers," IEEE J. Quantum Electron. **46**, 1860(2010).
19. J. Fini, "Design of large-mode-area amplifier fibers resistant to bend-induced distortion," J. Opt. Soc. Am. B **24**, 1669(2007).
20. N. Xia, and S. Yoo, "Mode instability in ytterbium-doped non-circular fibers," Opt. Express **25**, 13230(2017).
21. D. Marcuse, "Influence of curvature on the losses of doubly clad fibers," Appl. Opt. **21**, 4208(1982).
22. M.-Y. Cheng, Y.-C. Chang, A. Galvanauskas, P. Mamidipudi, R. Changkakoti, and P. Gatchell, "High energy and high peak power nanosecond pulse generation with beam quality control in 200-µm core highly multimode Yb-doped fiber amplifiers," Opt. Lett. **30**, 358(2005).
23. J. K. Sahu, S. Yoo, A. Boyland, C. Basu, M. Kalita, A. Webb, C. L. Sones, J. Nilsson, and D. N. Payne, "488 nm irradiation induced photodarkening study of Yb-doped aluminosilicate and phosphosilicate fibers," in Conference on Lasers and Electro-Optics/Quantum Electronics and Laser Science Conference and Photonic Applications Systems Technologies 2008, (Optical Society of America, 2008), paper JTuA27.
24. P. F. Moulton, G. A. Rines, E. V. Slobodtchikov, K. F. Wall, G. Frith, B. Samson, and A. L. G. Carter, "Tm-Doped Fiber Lasers: Fundamentals and Power Scaling," IEEE J. Sel. Top. Quantum Electron. **15**, 85(2009).
25. S. Yoo, A. S. Webb, A. J. Boyland, R. J. Standish, A. Dhar and J. K. Sahu, "Linearly polarized ytterbium-doped fiber laser in a pedestal design with aluminosilicate inner cladding," Laser Phys. Lett. **8**, 453(2011).
26. J. K. Sahu, S. Yoo, A. J. Boyland, A. Webb, C. Codemard, R. J. Standish, and J. Nilsson, "Ytterbium-doped low-NA P-Al-silicate large-mode-area fiber for high power applications," in Conference on Lasers and Electro-Optics/Quantum Electronics and Laser Science Conference and Photonic Applications Systems Technologies 2010, (Optical Society of America, 2010), CTuP3.
27. A. W. Snyder and W. R. Young, "Modes of optical waveguides," J. Opt. Soc. Am. **68**, 297 (1978).